Energy & Environmental Science

ROYAL SOCIETY OF CHEMISTRY

PAPER

View Article Online
View Journal | View Issue

Cite this: *Energy Environ. Sci.*, 2025, **18**, 937

Engineered biocatalytic architecture for enhanced light utilisation in algal H_2 production†

Sergey Kosourov, *[a] Tekla Tammelin [b] and Yagut Allahverdiyeva *[a]

Thin-layer photosynthetic biocatalysts (PBCs) offer an innovative and promising approach to the solar-powered generation of renewable chemicals and fuels. Thin-layer PBCs incorporate photosynthetic microbes, engineered for the production of targeted chemicals, into specifically tailored bio-based polymeric matrices. This unique integration forms a biocatalytic architecture that allows controlled distribution of light, nutrients, and substrates to the entrapped cells, optimising their performance. The research outlined in this study offers a systematic engineering approach to developing a biocatalytic architecture with improved light utilisation and enhanced photosynthetic conversion of captured light energy to molecular hydrogen (H_2), an important energy carrier and fuel. This was achieved by entrapping wild-type green alga *Chlamydomonas reinhardtii* and its mutants with truncated light-harvesting chlorophyll antenna (Tla) complexes within thin-layer (up to 330 μm-thick) polymeric matrices under sulphur-deprived conditions. Our step-by-step engineering strategy involved: (i) synchronising culture growth to select cells with the highest photosynthetic capacity for entrapment, (ii) implementing a photosynthetic antenna gradient in the matrix by placing Tla cells atop the wild-type algae for better light distribution, (iii) replacing the conventional alginate formulation with TEMPO-oxidised cellulose nanofibers for improved matrix stability and porosity, and (iv) employing a semi-wet production approach to simplify the removal of produced H_2 from the matrix with entrapped cells, thus preventing H_2 recycling. The engineered PBCs achieved a fourfold increase in H_2 photoproduction yield compared to conventional alginate films under the same irradiance (0.65 *vs.* 0.16 mol m^{-2} under 25 μmol photons m^{-2} s^{-1}, respectively) and maintained H_2 photoproduction activity for over 16 days. This resulted in a remarkable 4% light energy to hydrogen energy conversion efficiency at peak production activity and over 2% throughout the entire production period. These significant advancements highlight the potential of engineered thin-layer PBCs for efficient H_2 production. The technology could be adapted for biomanufacturing various renewable chemicals and fuels.

Received 12th July 2024,
Accepted 3rd December 2024

DOI: 10.1039/d4ee03075c

rsc.li/ees

Broader context

In the battle against climate change, the development of green technologies for the sustainable production of solar chemicals and fuels becomes essential as the demand for renewable energy sources intensifies. Among the most promising solutions are microalgae – tiny photosynthetic microorganisms capable of splitting water and producing H_2 gas using solar energy. However, applying microalgae on a large scale has proven challenging due to their low efficiency in utilising light, especially in dense cultures where light cannot penetrate deeply. This study introduces an innovative approach to overcoming these limitations by designing and manufacturing special thin-layer biocatalysts consisting of bio-based polymers with entrapped microalgae. By selectively entrapping the most efficient H_2-producing algal cells, specifically engineered for enhanced light distribution within the matrix, this research achieves a significant improvement in H_2 photoproduction compared to both suspension cultures and traditional immobilisation methods. The results provide a proof-of-concept for a novel technology in the biocatalytic production of solar H_2.

Introduction

Advancing emerging green technologies for the sustainable production of renewable chemicals and fuels is crucial for addressing climate change, reducing pollution, and achieving a zero-carbon society. In this direction, the application of

[a] *Molecular Plant Biology, Department of Life Technologies, University of Turku, FI-20014 Turku, Finland. E-mail: serkos@utu.fi, allahve@utu.fi*
[b] *VTT Technical Research Centre of Finland Ltd, VTT, PO Box 1000, FI-02044 Espoo, Finland*

† Electronic supplementary information (ESI) available. See DOI: https://doi.org/10.1039/d4ee03075c

microalgae, which utilise photosynthesis for light capture, CO_2 fixation, and solar chemical production, is of particular interest. However, one of the major bottlenecks to their broader incorporation in biotechnological applications is the low light utilisation efficiency in dense cultures. Like other photosynthetic microorganisms, microalgae possess large light-harvesting chlorophyll (Chl) antenna complexes, which enable individual algal cells to utilise light in low-light environments. However, this characteristic also presents a substantial challenge in the mass culturing of algae.[1] Within dense cultures, light intensity diminishes gradually in the direction opposite to the light source, conforming to the principles of light absorption by pigments outlined by the Bouguer–Beer–Lambert law and light scattering by cells.[2,3] Consequently, this phenomenon causes shading within the internal layers of the algal suspension, thereby constraining the overall photosynthetic productivity of the culture.

One potential solution to this challenge involves increasing the intensity of light directed towards the surface of the cultivation vessel or the photobioreactor (PBR).[4] This approach could be particularly useful for light-limiting conditions, such as lab-scale applications. Nonetheless, it is important to emphasise that the application of intense light may enhance photoinhibition in cells proximate to the PBR surface. Alternatively, another viable approach could involve reducing the optical path length of the PBR vessel, thereby facilitating greater light utilisation by the culture.[5] According to the available experimental data, optimal performance is achieved when the thickness of the PBR does not exceed 1 cm, considering typical culture densities.[6,7] Recent studies have demonstrated that the adoption of the thin-layer cultivation technique for highly concentrated algal cultures can markedly enhance the H_2 photoproduction yield under high irradiation.[8,9] However, implementing such a modification inevitably results in increased operational expenses for PBR cultivation, attributed to the additional resources needed for culture mixing and PBR construction.[1]

Another bottleneck to the widespread use of algae and other phototrophs, such as purple bacteria and cyanobacteria, as biocatalysts in chemical production is their constant growth, which leads to energy loss due to biomass formation. To address this issue, the whole-cell immobilisation approach has been proposed.[10–12] Entrapping algae within mechanically stable matrices limits cell division and significantly prolongs the biocatalytic activity of immobilised cells compared to those in suspension cultivation.[4,13] This method also minimises water usage and simplifies the process of exchanging media in the PBR, thereby facilitating periods of cell recovery and enabling multiple production cycles.[14,15]

Following the principle of thin-layer cultivation, our research group has devised an immobilisation strategy that distributes algae and cyanobacteria within thin polymeric matrices, up to 1 mm in thickness. These matrices are composed of alginate, TEMPO-oxidised cellulose nanofibers (TCNF), or a combination of both, and are cross-linked with Ca^{2+}, polyvinyl alcohol (PVA), or mixed-linkage glucan (MLG).[16,17] The research performed has demonstrated a significant advantage of employing thin-layer immobilisation in the photosynthetic production of H_2 and ethylene, as well as in the biotransformation of cyclohexanone to ε-caprolactone, using both green algae and cyanobacteria.[13,14,16,17] A similar enhancement has also been observed in the photosynthetic production of H_2 using thin latex coatings with entrapped cultures of purple non-sulphur bacteria, where the reactivity of the catalysts increased as the catalyst thickness decreased.[18,19]

In contrast to latex and other robust matrices used in whole-cell immobilisation,[12] the application of bio-based polymers like alginate and cellulose nanofibers offers additional advantages.[20,21] These include high compatibility with the hosted cells and biodegradability at the end of the application. Furthermore, bio-based polymers can be tailored for improved porosity and enhanced mechanical stability, making them suitable for use in additive manufacturing.[22] Thus, the assemblies of photosynthetic microbes, specifically engineered for the production of targeted chemicals, with specifically tailored bio-based polymers create a unique biocatalytic platform for solar chemical production.[21]

In this paper, we present a proof-of-concept for a novel architectural design of thin-layer photosynthetic biocatalysts (PBCs), specifically engineered to enhance light utilisation and boost H_2 photoproduction. This was achieved through a systematic bioengineering approach that optimises the spatial arrangement of green algae within the immobilisation matrix by creating a multi-layer architecture with a gradient of photosynthetic antennae. Additionally, the immobilisation matrix is tailored to facilitate the efficient release of H_2 from H_2-producing cells. Our approach significantly improves light capture efficiency and increases H_2 yield compared to traditional suspension cultures, while also dramatically extending the duration of the production process. Although this design focuses on enhancing photosynthetic H_2 production in green algae, the core principles of thin-layer engineering are broadly applicable. This framework could be adapted for the photosynthetic production of various solar chemicals and fuels across different photosynthetic organisms, as well as for application in artificial photosynthetic devices.

Results and discussion

Engineering the thin-layer biocatalytic architecture for improved light utilisation by H_2-producing algae has been performed following the strategy outlined in Scheme 1. The process involves four distinct steps, which are described below.

Engineering step #1: distribution of algae in thin films improves light utilisation

The initial engineering step (Scheme 1, step #1) involves employing a conventional thin-layer immobilisation approach, which has been widely adopted by our group and other research

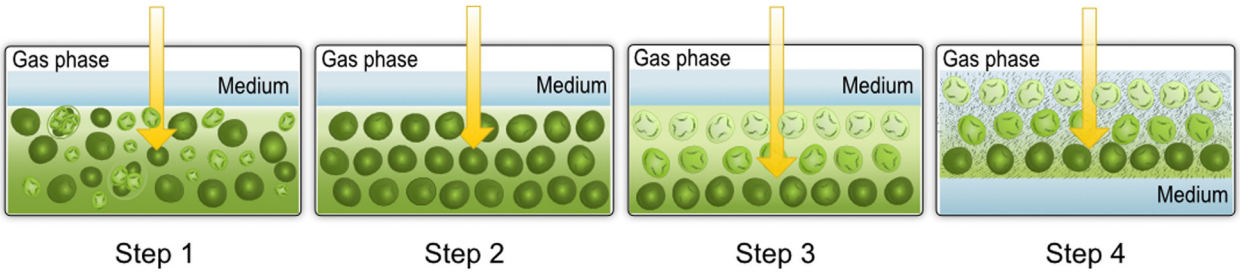

Scheme 1 Engineering strategy for improving light utilisation in thin-layer photosynthetic biocatalysts. Step 1: the conventional hydrogel film with low mechanical stability and porosity, containing a mixture of wild-type algal cells at various cell cycle stages. Step 2: introduction of synchronised algae harvested when they reach the maximum photosynthetic capacity. Step 3: introduction of a gradient of photosynthetic light-harvesting antenna truncation throughout the film with the smallest photosynthetic antenna cells at the top and the wild-type cells at the bottom of the film; algae are synchronised. Step 4: introduction of a matrix with improved porosity and mechanical stability; shifting H_2 production to the gas phase of the vials to facilitate H_2 release from films.

teams to enhance photosynthetic production of H_2 and other targeted chemicals and fuels.[13,15,18,23,24] Specifically, in the current work, we fabricated 180 μm-thick Ca^{2+}-alginate hydrogel films with entrapped wild-type cells of the green alga *Chlamydomonas reinhardtii*. These films were then subjected to sulphur deprivation (S-deprivation) to trigger sustained H_2 photoproduction.[23,25] In the absence of sulphur, algae gradually inactivate photosystem II (PS II)-dependent water oxidation activity, accumulate starch, and establish a microoxic environment due to nearly unchanged intracellular respiration.[26] This condition induces the expression of oxygen-sensitive [FeFe]-hydrogenase (H_2ase) in the algal chloroplast, leading to sustained H_2 photoproduction for a few days.

As shown in Fig. 1A (unsynchronised sample), the S-deprived algae entrapped within Ca^{2+}-alginate hydrogel films photoproduced H_2 for over 10 days, reaching the maximum activity of ~1 mmol H_2 m^{-2} h^{-1} between the fourth and fifth days. Cumulatively, the process yielded 0.16 mol H_2 per m^2 of the film surface. This corresponds to a 1.2% light energy to H_2 energy conversion efficiency (LHCE) in the photosynthetically active radiation (PAR) region, calculated at the maximum H_2 photoproduction rate, and 0.7% over the entire H_2 production period (Table 1, step #1). These values are close to one reported previously for 330 μm-thick Ca^{2+}-alginate films but exposed to slightly higher light (1.5% and 0.9%, respectively; under 60 μmol photons m^{-2} s^{-1} PAR).[23]

It is important to note that S-deprived suspension cultures of wild-type algae are capable of achieving similar LHCEs (both maximum and total values) only under conditions of intensive agitation in high-density cultivation.‡[7] In this scenario, production is primarily confined to a remarkably narrow photic zone, located proximal to the surface of the cultivation volume. However, the typical LHCE values in S-deprived suspensions rarely exceed 0.4%.[7,27] An additional advantage of thin-layer immobilisation is its ability to achieve maximum H_2 photoproduction activities and yields at significantly lower light intensities than suspensions. The research

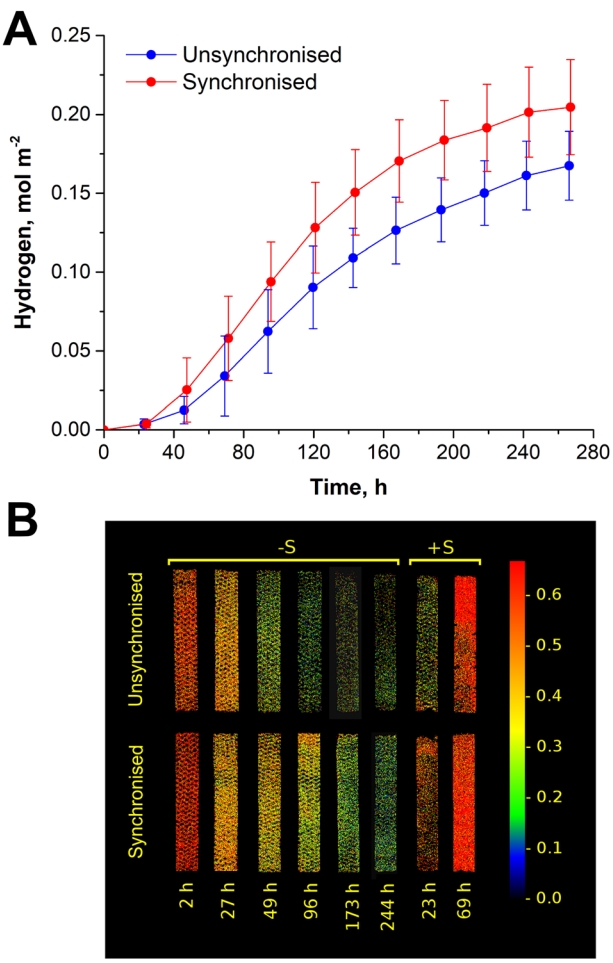

Fig. 1 Sustained H_2 photoproduction by 180 μm Ca^{2+}-alginate films with entrapped unsynchronised and synchronised cultures of green alga *C. reinhardtii* under S-deprived conditions. (A) H_2 photoproduction yields by films exposed to 25 μmol photons m^{-2} s^{-1} light. Values are the mean of 3 independent experiments with 18 (unsynchronised) and 20 (synchronised) vials in total ±SD. The paired *t*-test showed a significant difference between two datasets at $P < 0.001$. (B) False-colour Chl *a* fluorescence images of the films throughout S-deprivation (−S) and after shifting them to the medium containing normal amounts of sulphur (+ S). Fluorescence images of the films were taken after 5 minutes of dark adaptation and represent changes in the maximum efficiency of photosystem II (F_v/F_m) according to the colour scale on the right.

‡ The LHCE values provided in this reference were calculated using the upper H_2 gas combustion energy (ΔHc) of 285.8 kJ mol^{-1} and are noticeably overestimated relative to the data presented in the current work.

Table 1 Stepwise enhancement of the total H_2 photoproduction yield and LHCEs in the engineered thin-layer PBCs

	The total H_2 yield, mol m^{-2}	The maximum LHCE, %	The total LHCE, %[a]
Engineering step #1: submerged Ca^{2+}-alginate Wt film, unsynchronised	0.16 ± 0.02	1.2	0.7
Engineering step #2: submerged Ca^{2+}-alginate Wt film, synchronised	0.20 ± 0.03	1.9	0.9
Engineering step #3: submerged Ca^{2+}-alginate Tla2/Wt film, synchronised	0.45 ± 0.01	4.0	1.7
Engineering step #4: semi-wet Ca^{2+}-PVA-TCNF Tla2/Wt film, synchronised	0.65 ± 0.12	3.8	2.1

[a] The total LHCEs presented in the table were calculated for the period of 265 h for steps 1–3, and 385 h for step 4.

performed by Kosourov *et al.* at the National Renewable Energy Laboratory (Golden, CO, U.S.A.) has demonstrated that in 330 μm-thick films the process reaches saturation at around 30 μmol photons m^{-2} s^{-1} light.[28]

Engineering step #2: utilising synchronous algal cells with high photosynthetic capacity enhances light utilisation and increases photosynthetic production yield

In a wide range of biotechnological applications, including whole-cell immobilisation, the common practice involves the utilisation of unsynchronised cultures of photosynthetic microorganisms, which are typically cultivated under continuous illumination. These cultures comprise cells at various stages of the cell cycle (Scheme 1, step #1). In the context of a biocatalytic architecture, when unsynchronised cells are entrapped within a thin film (as described above), this heterogeneity intensifies light scattering and results in a non-uniform light and nutrient distribution throughout the immobilisation matrix. This condition creates an inhomogeneous environment within the matrix, distinguished by the presence of areas or 'niches' with different photosynthetic activities. It has been reported that such cellular heterogeneity plays a significant role in reducing the rate of H_2 production by S-deprived algae attached to glass textiles.[29,30] Therefore, for optimal performance, only uniform cells with superior photosynthetic capacity should be utilised in the fabrication of thin-layer PBCs. At the same time, the progression of the cell cycle in algae should be halted. This action redirects energy captured by photosynthesis from biomass formation towards H_2 photoproduction, thus preventing direct competition between CO_2 fixation and H_2 production pathways.[31–33]

In order to obtain the most competent cells for photosynthetic H_2 production, we synchronised *C. reinhardtii* cultures prior to immobilisation. Synchronous growth was achieved by alternating between light and dark periods (14 hours of light, followed by 10 hours of darkness).[34] In synchronised algal cultures, cell division predominantly occurs during the night.[35,36] With the onset of the first light, the daughter cells emerge from the mother cell and begin their growth phase, which continues throughout the light period. Consequently, young cells with a nascent photosynthetic apparatus initially exhibit low photosynthetic activity and enhanced respiration.[37] However, as the light period progresses, their photosynthetic activity increases, peaking approximately 4 to 6 h after the onset of illumination.[38,39] Photosynthetic activity then begins to decline due to starch accumulation and as the algal metabolism prepares for the upcoming cell division. Therefore, cells should be harvested during the phase of peak photosynthetic activity, but prior to reaching the commitment point after which the cell cycle can be completed with at least one division round.[40] When it comes to the second important requirement – arresting cell division, the entrapment of phototrophic cells in the immobilisation matrices might be sufficient in itself.[41] However, the effect could potentially be enhanced by employing sulphur deprivation, or deprivation by other nutrients, a recognised method for stopping cell division.[42,43] Most importantly, this condition is already utilised in this study to trigger sustained H_2 photoproduction. Therefore, we hypothesised that by immobilising *C. reinhardtii* cells harvested just before they reach their peak photosynthetic activity and subsequently depriving them of sulphur, we could effectively stabilise the algae in their most efficient biocatalytic state. The presence of such competent cells in the population of S-deprived algae has been indirectly confirmed by their cultivation in a two-stage sulphur-chemostat system.[44,45]

To further validate the above hypothesis, we constructed thin-layer Ca^{2+}-alginate biocatalysts using synchronously pre-grown wild-type *C. reinhardtii* cultures harvested 4 h post-illumination (Scheme 1, step #2). As shown in Fig. 1A, the synchronised algae, when entrapped in thin Ca^{2+}-alginate films, significantly outperformed the films with unsynchronised cells in terms of total H_2 photoproduction yield (0.20 *vs.* 0.16 mol H_2 m^{-2}, respectively) under S-deprived conditions. Most notably, Ca^{2+}-alginate films with entrapped synchronised cells demonstrated the maximum specific H_2 production rate of 5.04 μmol H_2 (mg Chl h)$^{-1}$, which was 1.7 times higher than the amount observed in unsynchronised samples (2.99 μmol H_2 (mg Chl h)$^{-1}$). As expected,[26,46] S-deprivation led to a gradual reduction in the maximum photochemical efficiency (F_v/F_m) of PSII in the entrapped algal cells. This reduction was visualised by the false-colour Chl *a* fluorescence images of the film surfaces, which represent changes in F_v/F_m, taken throughout the S-deprivation experiment (Fig. 1B, −S period). As shown in the figure, the loss of photochemical efficiency was less pronounced in biocatalysts with synchronised cells, which also exhibited a quicker recovery of PSII upon the re-addition of sulphur (Fig. 1B, +S period). Since the synchronised cultures were harvested near their peak photosynthetic performance before immobilisation, biocatalysts with entrapped synchronised algae had a higher average photosynthetic capacity at the onset of sulphur deprivation compared to those with unsynchronised cells. This initial advantage led to a slower decline in photochemical activity,

allowing for sustained H_2 production over a longer period (Fig. 1A). This data confirmed the conclusion by Volgusheva and co-authors that enhanced PSII stability during S-deprivation improves H_2 photoproduction yield in algae.[47] This indicates a direct dependence of the process on the residual PSII activity, as proposed in earlier research studies.[26,46] Furthermore, the accelerated recovery of films with synchronised cells upon sulphur re-addition at the end of the H_2 photoproduction cycle highlights the long-term effect of cell synchronisation (Fig. 1B, +S period).

As demonstrated in Table 1 (step #2), the synchronisation approach significantly enhanced the LHCE by Ca^{2+}-alginate films, which was close to 1.9% at the maximum H_2 photoproduction rate and reached 0.9% for the entire H_2 production period. These results emphasise the effectiveness of this engineering approach in optimizing light utilisation by immobilised *C. reinhardtii*. However, the immobilised algae still experienced light limitation, because the maximum specific activity in low cell density films with the same wild-type synchronised *C. reinhardtii* strain can exceed 12 μmol H_2 (mg Chl h)$^{-1}$,[23] showing room for further improvements.

Engineering step #3: application of the photosynthetic antenna gradient improves the overall light utilisation efficiency in the biocatalytic architecture

In an effort to optimise light distribution in mass cultures of green algae, a reduction in antenna size has been proposed.[48] This strategy aims to minimise energy wastage associated with non-photochemical quenching (NPQ) in the peripheral layers of the culture proximate to the light source, thus allowing for greater transmittance of irradiance through high-density cultivation. The proof-of-concept experiments demonstrated that algae with truncated photosynthetic antenna size do improve photosynthetic productivity under high light intensities,[49–51] and in particular, the H_2 photoproduction yield by S-deprived *C. reinhardtii* suspensions and alginate films.[52,53] However, this approach would not work in dense algal cultures exposed from low to intermediate irradiation (up to 200 μmol photons m^{-2} s^{-1}) due to low light utilisation by individual cells and enhanced light scattering in high-density cultivation.[52]

Here, we propose a multi-layer architecture with enhanced light distribution properties that would allow the algae-based photosynthetic biocatalyst to operate efficiently across a wide range of illumination conditions. In this approach (Scheme 1, step #3), a gradient of photosynthetic antenna truncation is established in the direction opposite to the light source by printing microalgal cells with the smallest photosynthetic antennae on the uppermost cell layers, while cells with larger antenna sizes are printed on the lower levels. This architecture would significantly decrease the dissipation of light energy in the upper layers of the film, making it more available to the lower layers. Consequently, this would lead to a substantial increase in the overall light utilisation efficiency.

To evaluate the benefits of the proposed architectural design, we fabricated biocatalysts consisting of the double-layer assembly of *C. reinhardtii* cells in Ca^{2+}-alginate matrix. In this sandwich-like architecture, the truncated antenna mutant, Tla2, was placed atop the wild-type algae with normal antenna size (Fig. 2A, Tla2/Wt film). Each layer was 180 μm thick. As a negative control, we created an architecture consisting of two layers of Tla2 (Fig. 2A, Tla2/Tla2 film). For the positive control, we applied two layers of wild-type cells (Fig. 2A, Wt/Wt film). It is important to note that the Tla2 mutant possesses a substantially lower Chl content per cell, corresponding to about 35% of photosynthetic antenna truncation compared to the corresponding wild-type control.[54] As mentioned above, the fabricated multi-layer PBCs were subjected to S-deprivation to initiate H_2 photoproduction.

As demonstrated in Fig. 2B, in all cases the double layer architecture with Tla2 cells atop showed significantly higher H_2 photoproduction yields compared to both controls. Most importantly, the effect was more pronounced in the synchronised algae (Fig. 2B). In the synchronised multi-layer PBCs, the H_2 photoproduction yield in the engineered Tla2/Wt architecture exceeded 0.4 mol H_2 m^{-2} with LHCE values slightly above

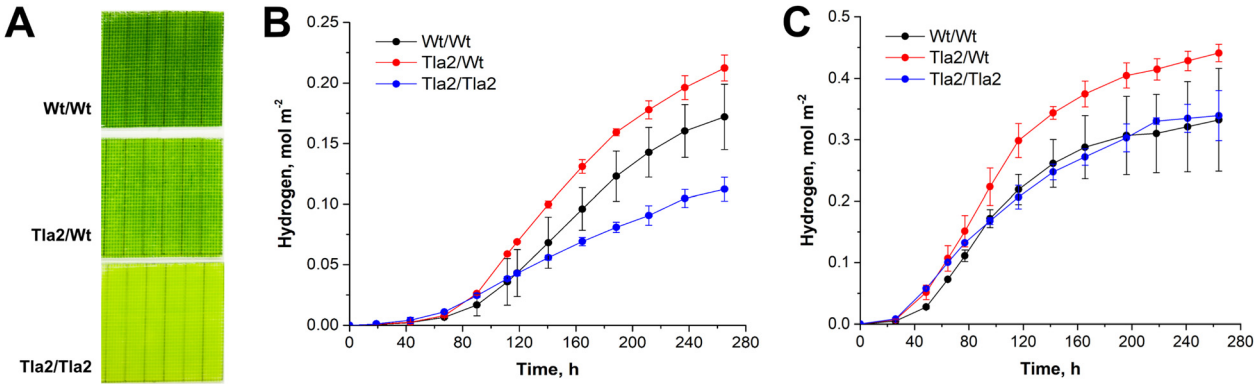

Fig. 2 The engineered biocatalytic architecture for improved light utilisation and H_2 photoproduction. (A) The engineered film with the truncated photosynthetic antenna mutant (Tla2) placed atop wild-type algae (Tla2/Wt film), along with its positive (Wt/Wt film) and negative (Tla2/Tla2 film) controls. (B) and (C) H_2 photoproduction yields by the films made of unsynchronised and synchronised algae, respectively. Values are the mean of three independent experiments ±SD. The paired *t*-test showed a significant difference between the Tla2/Wt architecture and both controls with *P* values below 0.01 (typically < 0.001) in both unsynchronised and synchronised films.

4% at the maximum H_2 photoproduction rate, and 1.7% over 265 h of H_2 production (Table 1, step #3).

Thus, by strategically selecting the most photosynthetically competent cells for immobilisation and engineering the biofilm properties to enhance light distribution, we achieved a synergistic enhancement in H_2 photoproduction. This led to a 2.8-fold increase in the total H_2 yield compared to conventional algal films. Consequently, the engineered films exhibited the highest LHCEs ever reported in S-deprived *C. reinhardtii* algae.

Engineering step #4: creating conditions for efficient removal of H_2 gas from the biocatalyst improves the overall H_2 production yield

H_2 production in algae, driven by the [FeFe]-H_2ase enzyme, is a highly reversible process. As a result, the H_2 photoproduction yield in sulphur-deprived algae depends on the partial pressure of H_2 and declines exponentially as H_2 accumulates in the cultures, shifting the equilibrium towards the back reaction.[55–57] This effect is even more pronounced in immobilised algae, where diffusion limitations within the immobilisation matrix significantly impact the specific H_2 photoproduction activity.[56]

To prevent the accumulation of H_2 within the thin-layer biocatalyst and decrease the probability of the reverse reaction, we transferred the production of H_2 from the liquid phase to the gas phase of the experimental vials by introducing a semi-wet production approach. In this approach, biocatalysts are placed on porous foam supports, which convey water and nutrients to the cells. These supports are positioned above the experimental medium to allow PBCs to be directly exposed to an atmosphere initially filled with 100% argon at the beginning of the experiment. Experiments with single-layer Ca^{2+}-alginate films containing S-deprived algae demonstrated a significant improvement in H_2 photoproduction yields in semi-wet films compared to submerged films (ESI,† Fig. S1). Notably, the effect was most pronounced in films with synchronised algae (ESI,† Fig. S1).

At this stage of engineering, we also replaced the matrix formulation from alginate to TEMPO-oxidised cellulose nanofibers (TCNF). Nanocellulose-based matrices offer superior mechanical stability compared to alginate formulations, prevent matrix disintegration under challenging experimental conditions, provide better porosity, and show potential for tailoring to desired properties.[16,17,58,59] The S-deprived algal films made of TEMPO-oxidized cellulose nanofibers cross-linked with Ca^{2+} and polyvinyl alcohol (Ca^{2+}-PVA-TCNF films) demonstrated similar H_2 yields compared to the Ca^{2+}-alginate films (ESI,† Fig. S2). Therefore, in our final experiment, we fabricated double-layer Ca^{2+}-PVA-TCNF films with entrapped synchronised *C. reinhardtii* algae. These films consisted of 120 μm-thick Tla2 and Wt layers (with Tla2 on top of Wt), representing the final architectural design of thin-layer PBCs with improved light utilisation (Scheme 1, step #4). We also included two controls: 240 μm-thick Wt/Wt (positive) and Tla2/Tla2 (negative) films made of the same TCNF formulation.

Similar to the data obtained at step #3, the application of the Tla2/Wt architecture in the TCNF matrix significantly improved

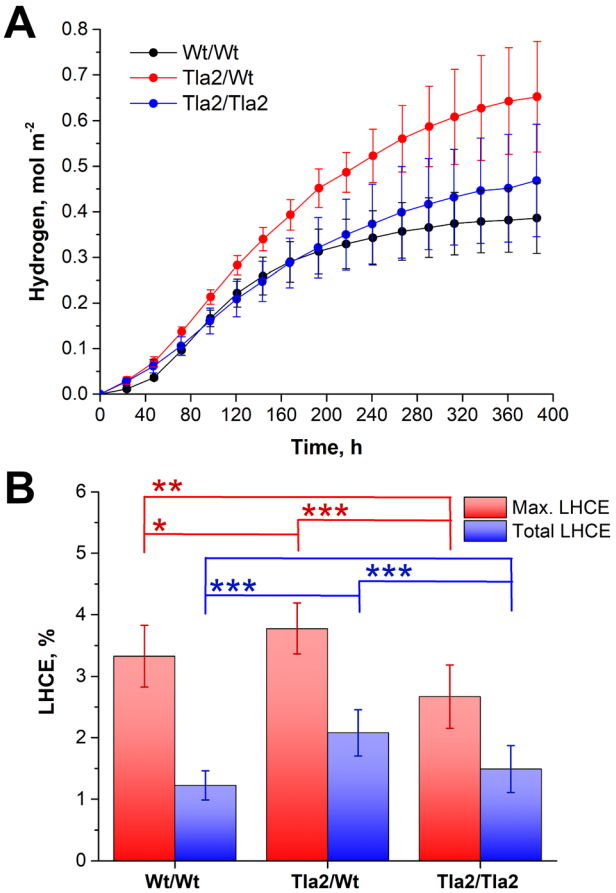

Fig. 3 Application of an engineered biocatalytic architecture with improved light distribution within a nanoporous Ca^{2+}-PVA-TCNF matrix for semi-wet H_2 production. (A) H_2 photoproduction yields by the films, and (B) corresponding LHCEs calculated for the maximum production activity and the total H_2 production period. Abbreviations for the film architecture are the same as in Fig. 2. Values are the mean of four independent experiments ± SD. The differences in H_2 yields are significant at $P < 0.01$. For LHCE values, significant differences are indicated as follows: *$P < 0.05$; **$P < 0.01$; ***$P < 0.001$.

the H_2 photoproduction yield compared to both controls (Fig. 3A), and the effect was amplified by semi-wet production conditions (compare H_2 production yields in Fig. 2C and 3A). However, the semi-wet cultivation approach did not enhance the maximum H_2 photoproduction activity of the immobilized algae. This resulted in a similar maximum LHCE for the engineered Tla2/Wt Ca^{2+}-PVA-TCNF films under semi-wet production conditions and their Ca^{2+}-alginate counterparts under submerged cultivation conditions (compare maximum LHCEs for steps #3 and #4 in Table 1). Nevertheless, the semi-wet approach prolonged the duration of H_2 production activity in all engineered films, resulting in an impressive 2.1% LHCE over the entire 385 h (~16 d) H_2 production period (Table 1, step #4). During this period, the Tla2/Wt PBCs produced nearly 0.65 mol H_2 m^{-2}, which is significantly higher than the best scenario reported for suspension cultures of S-deprived wild-type algae by Giannelli *et al.*,[7] who observed approximately 0.15 mol H_2 per m^{-2} of the illuminated surface of a

photobioreactor (146 mL H_2 $L_{culture}^{-1}$). On average, the engineered Tla2/Wt PBCs yielded approximately 960 mL H_2 per liter of TAP medium. It is important to note that some photosynthetic mutants have been reported to produce 500–850 mL H_2 $L_{culture}^{-1}$ under S-deprived conditions.[60–62] However, these studies do not provide information on the photobioreactor geometry or LHCE values, making it impossible to directly compare areal H_2 productivities with our system. Nonetheless, the application of these mutants within the engineered architecture has the potential to further enhance LHCE.

It should also be noted that the S-deprivation approach used in this study to induce H_2 production in algae has limitations for the long-term performance of PBCs. In the absence of sulphur, recovery of PSII reaction centres in cells is impaired, meaning subsequent cycles of H_2 production are only feasible after a few days of the biocatalyst recovery in the sulphur-replete medium. In this regime, however, conventional PBCs have been shown to produce H_2 for more than 150 days (~5 months), although the most efficient H_2 photoproduction is achieved during the initial production cycle.[4] Even within a single production cycle, 1 m^2 PBCs with the double-layer architecture can generate ~42 W h of energy stored as H_2 over 16 days. If effectively converted to electricity, this technology holds the potential for powering small-scale IoT devices and remote sensors. However, practical implementation will depend greatly on advancements in efficient, compact, and affordable fuel cells to effectively convert H_2 for small-scale use.

An alternative to S-deprivation could be recently developed methods such as pulse-illumination and CO_2 limitation.[31,32] These approaches help prevent activation/functioning of the Calvin–Benson–Bassham (CBB) cycle, thereby reducing competition with H_2ase for photosynthetic electrons. Importantly, they achieve this without the significant damage to the photosynthetic apparatus often observed in nutrient deprivation approaches.[26,63] A recent proof-of-concept study by Kanygin *et al.*[64] demonstrated that competition with CO_2 fixation in the CBB cycle can be effectively avoided by directly fusing H_2ase with photosystem I, allowing more effective channelling of photosynthetic electrons toward H_2 production. This approach has shown promise for sustaining long-term H_2 photoproduction in algal cultures, achieving a maximum LHCE of up to 1.75% (although measured under 630-nm monochromatic light). While effective in suspension cultures, the methods for preventing competition with the CBB cycle have yet to be tested in immobilized systems. In terms of areal productivity, our engineered PBCs exhibit significantly higher performance compared to suspension cultures. For instance, our calculations based on Nagy's *et al.*[9] data showed that thin-layer, CO_2-limited cultures yield approximately 0.1 mol H_2 per m^2 of illuminated area for the wild-type CC-124 strain and around 0.2 mol H_2 per m^2 for the pgr5 mutant in the long-term (144 h) process (compared with 0.65 mol H_2 m^{-2} over 385 h in Fig. 3A).

We also evaluated the performance of a triple-layer architecture comprising Tla3 (or Tla5) cells with nearly 60% truncated photosynthetic antennae,[65] placed atop the Tla2 layer, and followed by a layer of wild-type cells. Each layer was 80 μm thick, resulting in the total film thickness of 240 μm. This architecture showed improved performance only under high light intensities (ESI,† Fig. S3) due to significantly reduced H_2 photoproduction activity in Tla3 and Tla5 strains. The latter is likely caused by a significant loss of photosynthetic reaction centres in Δ*cpsrp*43 *tla* mutants, both PSII and PSI.[65] It is important to note that while this top layer does not produce H_2 efficiently, it competes for acetate with other cells during the initial hours of S-deprivation, when algae primarily accumulate starch. The inability to accumulate starch under low light conditions leads to an inability to sustain the H_2 production activity in the later stages of S-deprivation.[66,67] Nevertheless, the enhanced performance of the triple-layer architecture under high light (though with a lower H_2 yield than under low light) suggests that this particular design, incorporating Tla3 and Tla5 mutants, would be more suitable for producing other chemicals rather than H_2.

Conclusions

This study presents a systematic engineering approach to developing PBCs for efficient light utilisation and H_2 photoproduction using green algae entrapped within thin polymeric matrices. By synchronising algal growth and selecting cells with the highest photosynthetic capacity for entrapment, implementing a photosynthetic antenna gradient to enhance light distribution throughout the matrix, introducing Ca^{2+}-PVA-TCNF matrix with improved physical properties, and enhancing the removal of produced H_2 from the biocatalyst by employing the semi-wet cultivation approach, we achieved a fourfold increase in the H_2 photoproduction yield compared to conventional Ca^{2+}-alginate films with unsynchronised algae under the same irradiance. As a result, the engineered H_2-producing biocatalytic architecture demonstrated an impressive 4% LHCE at peak production activity and over 2% throughout an extended H_2 production period of 385 hours. These results highlight the potential of engineered PBCs for sustainable and efficient solar H_2 production. Furthermore, the engineering approach devised and implemented in this study holds promise for enhancing the production of other solar chemicals and fuels.

Experimental

Strains and growth conditions

The wild-type green alga *C. reinhardtii* (strain CC-124) and truncated light-harvesting Chl antenna mutants Tla2 (strain CC-4476), Tla3 (strain CC-4561), and Tla5 (strain CC-4475) were obtained from the Chlamydomonas Resource Center at the University of Minnesota, USA. Fig. 4 describes some unique properties of Tla mutants.

Stock cultures were maintained photoheterotrophically in 150 mL Erlenmeyer flasks containing 50 mL of standard Tris-acetate-phosphate (TAP) medium. The flasks were placed on a shaker (~100 rpm) illuminated with cool-white fluorescent lamps that provided around 30 μmol photons m^{-2} s^{-1} at the

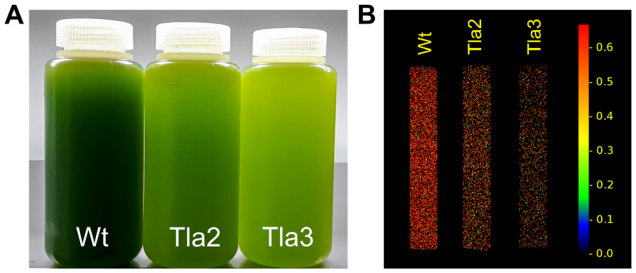

Fig. 4 Comparison of (A) light penetration within cultures of wild-type, Tla2, and Tla3 strains with similar cell densities, and (B) their photochemical activity, shown as false-colour Chl *a* fluorescence images of Ca^{2+}-alginate films taken 2 hours after immobilisation. Fluorescence images represent changes in F_v/F_m according to the colour scale on the right. The Tla5 mutant behaves similarly to Tla3.

top of the flasks. For normal growth, cultures were cultivated at 25 °C and diluted weekly with fresh medium. The synchronous growth was achieved by alternating light (14 h) and dark (10 h) periods and maintained by daily dilution of the cultures.[34,43] Synchronisation was monitored through periodic sampling and visualisation of algae in a haemocytometer under a microscope. Cells harvested at the end of the 24-hour cycle (1–2 hours before the onset of illumination) displayed distinct morphological characteristics. At this time, the culture predominantly consisted of uniform zoospores enclosed within parental cell walls, indicating successful synchronisation.[68,69]

The experimental cultures were started from diluted stock cultures and grown at 25 °C in 1 L Roux bottles containing 700 mL TAP medium. During growth, the cultures were continuously bubbled with sterile 2% CO_2 in air (photomixotrophic growth) using 0.2 μm pore-size membrane filters (Acro 37 TF, Gelman Sciences, Inc., USA) and illuminated from one side with 75 μmol photons m^{-2} s^{-1} of cool-white fluorescent light. For synchronous growth, the cultures were grown under a 14 h photoperiod. Prior to immobilisation, cultures at the late logarithmic phase (20–25 μg total Chl mL^{-1}) were harvested by centrifugation at 3000*g* for 3 min, washed once in TAP-minus-sulphur-minus-phosphorus (TAP-S-P) medium to remove sulphates and phosphates, and pelleted again by centrifugation. Phosphorus exclusion in addition to S-deprivation was necessary for stabilisation of the films but did not affect H_2 production in algae.[23]

Preparation of single- and double-layer Ca^{2+}-alginate films

The films were prepared using a formulation ratio of 1 g of wet cell biomass, 0.5 mL of water, and 1 mL of 4% sodium alginate (#71238, Sigma-Aldrich) under sterile conditions. The mixture was manually coated onto the surface of the template, which consisted of a polymer insect screen placed over the sticky side of a wide strip of Scotch-type tape.[13,23] This was done using a sterile glass pipette to form a microfilm. Gelation of the film was initiated by spraying the surface with a 50 mM $CaCl_2$ solution. In this approach, the thickness of the alginate films was approximately 180 μm and was influenced by the thickness of the plastic insect screen used as mechanical support. Double-layer 360 μm films were prepared by coating a second layer atop the first before the application of $CaCl_2$. The insect screen was not used in the second layer. Instead, the required thickness was achieved by using spacers on the sides during coating. This fabrication approach provided sufficient mechanical stability for the film during its submerged cultivation.

Preparation of Ca^{2+}-PVA-TCNF films with multilayer architecture for the semi-wet H_2 production

TEMPO-oxidised cellulose nanofibers (TCNF), derived from never-dried bleached softwood pulp obtained from a Finnish pulp mill, were utilised in the preparation of multilayer films for semi-wet H_2 production. The TEMPO-catalysed oxidation of pulp fibres was conducted as described by Saito *et al.*[70] 2,2,6,6-Tetramethylpiperidine-1-oxyl (TEMPO, Sigma-Aldrich) and 10% sodium hypochlorite (5 mmol g^{-1} pulp fibres) were used in the TEMPO-catalysed oxidation of the pulp. The oxidised pulp was washed and passed twice through a microfluidiser (Microfluidics Int., USA) equipped with two Z-type chambers with diameters of 400 and 100 μm at 1850 bar to fibrillate the oxidised pulp into TCNF with a final consistency of ~1 wt% and anionic charge of ~1.5 mmol g^{-1}. The chemical composition, charge, morphology and visual outlook of similarly prepared TCNF-grade used in this study have been described in our previous publications.[16,58,59] For semi-wet cultivation, the films were coated on 300 μm-thick blotting paper supports, which were used as both a mechanical support and a porous material to distribute water and nutrients to the entrapped cells through capillary action. The 120 μm-thick layers (double-layer films) and 80 μm-thick layers (triple-layer films) were formed from a formulation consisting of algal biomass mixed in 1 : 1 wet mass ratio with 1 wt% TCNF and 0.1 wt% PVA (Mowiol® 56–98, M_w ~ 195 000 g mol^{-1}, DP 4300, Sigma-Aldrich), as previously described.[16,59] The films were coated layer-by-layer using an automatic film applicator (TQC Sheen) and spacers of the required thickness. Finally, the multilayer films were treated by spraying 50 mM $CaCl_2$ over the surface of the film to maintain consistency with the preparation of alginate films.[16,23,59]

H_2 photoproduction experiments

The fabricated films were washed in Milli-Q water and cut into 6 × 1 cm strips. For submerged cultivation, the strips were placed in 10 mL TAP-S-P medium in 75 mL gas-tight vials. For semi-wet cultivation, the strips were placed on the surface of a water-conveying 6 × 1 × 1 cm melamine foam support inside the same vials, ensuring the strips remained above the 10 mL TAP-S-P medium. The vials were sealed with butyl rubber stoppers, and the gas phase within the vials was replaced with pure argon. The H_2 and O_2 contents in the headspace of the vials were monitored daily using a gas chromatograph (Clarus 500, PerkinElmer, Inc.) equipped with a thermal conductivity detector and a molecular sieve 5A column (60/80 mesh). The amounts of H_2 and O_2 dissolved in the liquid phase were calculated based on the partial pressure of each gas at the time of sampling and their respective solubility coefficients.

These values, along with the quantities of gases withdrawn for sampling, were considered in the final production yields. The maximum specific H_2 production rates were calculated based on the initial total Chl (a + b) content in the films. The chlorophyll content was determined spectrophotometrically, as previously described.[71]

Calculation of light energy to H_2 energy conversion efficiency

The average irradiance (W m^{-2}) at the surface of the films from the incident light in the PAR (400–700 nm) region was determined using a handheld portable spectroradiometer (SpectraPen LM 500, PSI, Czech Republic). LHCE were calculated using the eqn (1), which considers the partial pressure of H_2 gas in the vial headspace at the moment of calculation:

$$\eta\ (\%) = 100 \times \frac{\left(\Delta G^{\circ} - RT\ln\left(\frac{P^{\circ}}{P}\right)\right) R_{\mathrm{H}}}{E_{\mathrm{s}} A} \qquad (1)$$

where ΔG° is the change of the standard Gibb's free energy for the water-splitting reaction (237200 J mol^{-1} at 25 °C and 1 atm), R is the universal gas constant (8.3145 J K^{-1} mol^{-1}), T is the absolute temperature (K), P° and P are standard and observed H_2 pressures (atm), R_{H} is the rate of H_2 photoproduction (mol s^{-1}), E_{S} is the energy of the incident light radiation (J m^{-2} s^{-1}), and A is the illuminated surface area (m^2).

Chl *a* fluorescence imaging

Chl a fluorescence images of the film surface were obtained at 22 °C under aerobic conditions using an imaging fluorometer (FluorCam FC-800-O/1010, PSI, Czech Republic). The films were extracted from the vials, adapted in the dark for 5 minutes, and placed in the center of the measuring unit. Fluorescence images were captured at F_0 (2 s after the start of the protocol) and F_{m} (induced by an 800 ms saturating royal-blue pulse of ~2000 μmol photons m^{-2} s^{-1} applied 5 s after the start of the protocol). The $F_{\mathrm{v}}/F_{\mathrm{m}}$ values were calculated from the F_0 and F_{m} images as $(F_{\mathrm{m}} - F_0)/F_{\mathrm{m}}$ using FluorCam 7.0 software.

Author contributions

Conceptualization and methodology SK, YA; methodology and provision of TCNF formulations TT; investigation and data analysis SK; resources all authors; writing – original draft SK; writing – review & editing all authors.

Data availability

The data supporting this article have been included as part of the ESI.†

Conflicts of interest

There are no conflicts to declare.

Acknowledgements

The authors would like to express their gratitude to Prof. Anastasios Melis and his team for their work in developing the light-harvesting photosynthetic antenna mutants and for making them accessible to the research community through the Chlamydomonas Resource Center. We also thank Dr Fiona Lynch for her assistance with film imaging. This work was financially supported by the Maj and Tor Nessling Foundation (project no. 201400050), the Novo Nordisk Foundation (Nanoplatform, project no NNF16OC0021626), the Kone Foundation (project no. 201608799), the NordForsk Nordic Center of Excellence ''NordAqua'' (project no. 82845), the EU FET Open Project FuturoLEAF under grant agreement no. 899576, and the Research Council of Finland (AlgaLEAF, project no. 322752 and 322754). The work is part of Research Council of Finland's Flagship Programme FinnCERES, Competence Center for Materials Bioeconomy. The research was performed in the PhotoSYN Finnish Infrastructure for Photosynthesis Research.

Notes and references

1 G. Torzillo, B. Pushparaj, J. Masojidek and A. Vonshak, *Biotechnol. Bioprocess Eng.*, 2003, **8**, 338–348.
2 J.-F. Cornet, C. G. Dussap, J.-B. Gros, C. Binois and C. Lasseur, *Chem. Eng. Sci.*, 1995, **50**, 1489–1500.
3 L. Pottier, J. Pruvost, J. Deremetz, J.-F. Cornet, J. Legrand and C. G. Dussap, *Biotechnol. Bioeng.*, 2005, **91**, 569–582.
4 S. N. Kosourov, M. He, Y. Allahverdiyeva and M. Seibert, *Microalgal Hydrogen Production: Achievements and Perspectives*, The Royal Society of Chemistry, 2018, pp. 355–384.
5 J. Pruvost, F. Le Borgne, A. Artu and J. Legrand, *Algal Res.*, 2017, **21**, 120–137.
6 N. Zou and A. Richmond, *J. Biotechnol.*, 1999, **70**, 351–356.
7 L. Giannelli, A. Scoma and G. Torzillo, *Biotechnol. Bioeng.*, 2009, **104**, 76–90.
8 J. Liu, V. Bukatin and A. Tsygankov, *Int. J. Hydrogen Energy*, 2006, **31**, 1591–1596.
9 V. Nagy, A. Podmaniczki, A. Vidal-Meireles, S. Kuntam, É. Herman, L. Kovács, D. Tóth, A. Scoma and S. Z. Tóth, *Bioresour. Technol.*, 2021, **333**, 125217.
10 S. F. Karel, S. B. Libicki and C. R. Robertson, *Chem. Eng. Sci.*, 1985, **40**, 1321–1354.
11 R. Willaert, *Encyclopedia of Industrial Biotechnology*, John Wiley & Sons, Inc., Hoboken, NJ, USA, 2009.
12 A. Léonard, P. Dandoy, E. Danloy, G. Leroux, C. F. Meunier, J. C. Rooke and B.-L. Su, *Chem. Soc. Rev.*, 2011, **40**, 860–885.
13 H. Leino, S. N. Kosourov, L. Saari, K. Sivonen, A. A. Tsygankov, E. M. Aro and Y. Allahverdiyeva, *Int. J. Hydrogen Energy*, 2012, **37**, 151–161.
14 S. Kosourov, H. Leino, G. Murukesan, F. Lynch, K. Sivonen, A. A. Tsygankov, E.-M. Aro and Y. Allahverdiyeva, *Appl. Environ. Microbiol.*, 2014, **80**, 5807–5817.
15 H. Lee, D. Shin, J. Choi, C. S. Ki and J. Hyun, *Carbohydr. Polym.*, 2022, **290**, 119485.

16 M. Jämsä, S. Kosourov, V. Rissanen, M. Hakalahti, J. Pere, J. A. Ketoja, T. Tammelin and Y. Allahverdiyeva, *J. Mater. Chem. A*, 2018, **6**, 5825–5835.
17 T. Virkkala, S. Kosourov, V. Rissanen, V. Siitonen, S. Arola, Y. Allahverdiyeva and T. Tammelin, *J. Mater. Chem. B*, 2023, **11**, 8788–8803.
18 J. L. Gosse, B. J. Engel, F. E. Rey, C. S. Harwood, L. E. Scriven and M. C. Flickinger, *Biotechnol. Prog.*, 2007, **23**, 124–130.
19 J. L. Gosse, B. J. Engel, J. C.-H. Hui, C. S. Harwood and M. C. Flickinger, *Biotechnol. Prog.*, 2010, **26**, 907–918.
20 N. Mallick, *Biometals Int. J. Role Met. Ions Biol. Biochem. Med.*, 2002, **15**, 377–390.
21 K. Heise, E. Kontturi, Y. Allahverdiyeva, T. Tammelin, M. B. Linder, Nonappa and O. Ikkala, *Adv. Mater.*, 2021, **33**, 2004349.
22 G. S. Tóth, O. Backman, T. Siivola, W. Xu, S. Kosourov, V. Siitonen, C. Xu and Y. Allahverdiyeva, *Green Chem.*, 2024, **26**, 4032–4042.
23 S. N. Kosourov and M. Seibert, *Biotechnol. Bioeng.*, 2009, **102**, 50–58.
24 V. Siitonen, A. Probst, G. Tóth, R. Kourist, M. Schroda, S. Kosourov and Y. Allahverdiyeva, *Green Chem.*, 2023, **25**, 5945–5955.
25 A. Melis, L. Zhang, M. Forestier, M. L. Ghirardi and M. Seibert, *Plant Physiol.*, 2000, **122**, 127–136.
26 L. Zhang, T. Happe and A. Melis, *Planta*, 2002, **214**, 552–561.
27 M. L. Ghirardi, *Indian J. Biochem. Biophys.*, 2006, **43**, 201–210.
28 M. L. Ghirardi, *Algal Systems for Hydrogen Photoproduction*, Golden Field Office, Golden, CO (United States), 2015.
29 T. V. Laurinavichene, A. S. Fedorov, M. L. Ghirardi, M. Seibert and A. A. Tsygankov, *Int. J. Hydrogen Energy*, 2006, **31**, 659–667.
30 T. V. Laurinavichene, S. N. Kosourov, M. L. Ghirardi, M. Seibert and A. A. Tsygankov, *J. Biotechnol.*, 2008, **134**, 275–277.
31 S. Kosourov, M. Jokel, E.-M. Aro and Y. Allahverdiyeva, *Energy Environ. Sci.*, 2018, **11**, 1431–1436.
32 V. Nagy, A. Podmaniczki, A. Vidal-Meireles, R. Tengölics, L. Kovács, G. Rákhely, A. Scoma and S. Z. Tóth, *Biotechnol. Biofuels*, 2018, **11**, 69.
33 S. Vajravel, Y. Allahverdiyeva and S. Kosourov, *Sustainable Energy Fuels*, 2023, **7**, 1818–1828.
34 S. Kosourov, A. Tsygankov, M. Seibert and M. L. Ghirardi, *Biotechnol. Bioeng.*, 2002, **78**, 731–740.
35 J. M. Zones, I. K. Blaby, S. S. Merchant and J. G. Umen, *Plant Cell*, 2015, **27**, 2743–2769.
36 E. H. Harris, *The Chlamydomonas sourcebook: a comprehensive guide to biology and laboratory use*, Academic Press, San Diego, 1989.
37 T. Ehara, T. Osafune and E. Hase, *J. Cell Sci.*, 1995, **108**, 499–507.
38 D. Kaftan, T. Meszaros, J. Whitmarsh and L. Nedbal, *Plant Physiol.*, 1999, **120**, 433–442.
39 H. Senger and N. I. Bishop, *Planta*, 1979, **145**, 53–62.
40 H. Oldenhof, V. Zachleder and H. van den Ende, *Folia Microbiol.*, 2007, **52**, 53–60.
41 D. Dickson, C. Page and R. Ely, *Int. J. Hydrogen Energy*, 2009, **34**, 204–215.
42 E. Hase, H. Otsuka, S. Mihara and H. Tamiya, *Biochim. Biophys. Acta*, 1959, **35**, 180–189.
43 A. Tsygankov, S. Kosourov, M. Seibert and M. L. Ghirardi, *Int. J. Hydrogen Energy*, 2002, **27**, 1239–1244.
44 S. Kosourov, M. L. Ghirardi and M. Seibert, *US Pat.*, US7732174B2, 2010.
45 A. S. Fedorov, S. Kosourov, M. L. Ghirardi and M. Seibert, *Appl. Biochem. Biotechnol.*, 2005, **121–124**, 403–412.
46 T. K. Antal, T. E. Krendeleva, T. V. Laurinavichene, V. V. Makarova, M. L. Ghirardi, A. B. Rubin, A. A. Tsygankov and M. Seibert, *Biochim. Biophys. Acta, Bioenerg.*, 2003, **1607**, 153–160.
47 A. Volgusheva, S. Styring and F. Mamedov, *Proc. Natl. Acad. Sci. U. S. A.*, 2013, **110**, 7223–7228.
48 A. Melis, *Plant Sci.*, 2009, **177**, 272–280.
49 A. Melis, J. Neidhardt and J. R. Benemann, *J. Appl. Phycol.*, 1998, **10**, 515–525.
50 J. E. W. Polle, S.-D. Kanakagiri and A. Melis, *Planta*, 2003, **217**, 49–59.
51 H. Kirst and A. Melis, *Microalgal Hydrogen Production*, 2018, pp. 335–354.
52 S. N. Kosourov, M. L. Ghirardi and M. Seibert, *Int. J. Hydrogen Energy*, 2011, **36**, 2044–2048.
53 M. Oey, I. L. Ross, E. Stephens, J. Steinbeck, J. Wolf, K. A. Radzun, J. Kügler, A. K. Ringsmuth, O. Kruse and B. Hankamer, *PLoS One*, 2013, **8**, e61375.
54 H. Kirst, J. G. García-Cerdán, A. Zurbriggen and A. Melis, *Plant Physiol.*, 2012, **158**, 930–945.
55 T. S. Stuart and H. Gaffron, *Plant Physiol.*, 1972, **50**, 136–140.
56 S. N. Kosourov, K. A. Batyrova, E. P. Petushkova, A. A. Tsygankov, M. L. Ghirardi and M. Seibert, *Int. J. Hydrogen Energy*, 2012, **37**, 8850–8858.
57 A. Scoma and A. Hemschemeier, *Algal Res.*, 2017, **26**, 341–347.
58 V. Rissanen, S. Vajravel, S. Kosourov, S. Arola, E. Kontturi, Y. Allahverdiyeva and T. Tammelin, *Green Chem.*, 2021, **23**, 3715–3724.
59 T. Levä, V. Rissanen, L. Nikkanen, V. Siitonen, M. Heilala, J. Phiri, T. C. Maloney, S. Kosourov, Y. Allahverdiyeva, M. Mäkelä and T. Tammelin, *Biomacromolecules*, 2023, **24**, 3484–3497.
60 O. Kruse, J. Rupprecht, K.-P. Bader, S. Thomas-Hall, P. M. Schenk, G. Finazzi and B. Hankamer, *J. Biol. Chem.*, 2005, **280**, 34170.
61 G. Torzillo, A. Scoma, C. Faraloni, A. Ena and U. Johanningmeier, *Int. J. Hydrogen Energy*, 2009, **34**, 4529–4536.
62 J. Steinbeck, D. Nikolova, R. Weingarten, X. Johnson, P. Richaud, G. Peltier, M. Hermann, L. Magneschi and M. Hippler, *Front. Plant Sci.*, 2015, **6**, 1–11.
63 M. E. Sáenz, K. Bišová, E. Touloupakis, C. Faraloni, W. D. Di Marzio and G. Torzillo, *Int. J. Hydrogen Energy*, 2015, **40**, 10410–10417.
64 A. Kanygin, Y. Milrad, C. Thummala, K. T. Reifschneider, P. Baker, P. Marcu, I. Yacoby and K. E. Redding, *Energy Environ. Sci.*, 2020, **13**, 2903–2914.
65 H. Kirst, J. G. Garcia-Cerdan, A. Zurbriggen, T. Ruehle and A. Melis, *Plant Physiol.*, 2012, **160**, 2251–2260.

66 S. Fouchard, A. Hemschemeier, A. Caruana, J. Pruvost, J. Legrand, T. Happe, G. Peltier and L. Cournac, *Appl. Environ. Microbiol.*, 2005, **71**, 6199–6205.
67 A. Hemschemeier, S. Fouchard, L. Cournac, G. Peltier and T. Happe, *Planta*, 2008, **227**, 397–407.
68 A. J. Molendijk, P. Van Egmond, M. A. Haring, F. M. Klis and H. Van Den Ende, *J. Gen. Microbiol.*, 1992, **138**, 1941–1947.
69 W. Pokora, A. Aksmann, A. Baścik-Remisiewicz, A. Dettlaff-Pokora and Z. Tukaj, *J. Plant Physiol.*, 2018, **230**, 61–72.
70 T. Saito, Y. Nishiyama, J.-L. Putaux, M. Vignon and A. Isogai, *Biomacromolecules*, 2006, **7**, 1687–1691.
71 S. Kosourov, G. Murukesan, M. Seibert and Y. Allahverdiyeva, *Algal Res.*, 2017, **28**, 253–263.